BIOCHEMISTRY
including biophysical chemistry & molecular biology

Article

pubs.acs.org/biochemistry

Structure and Dynamics of Small Soluble Aβ(1−40) Oligomers Studied by Top-Down Hydrogen Exchange Mass Spectrometry

Jingxi Pan,[†] Jun Han,[‡] Christoph H. Borchers,[‡] and Lars Konermann*,[†]

[†]Department of Chemistry, The University of Western Ontario, London, Ontario N6A 5B7, Canada

[‡]University of Victoria-Genome BC Proteomics Centre, Victoria, British Columbia V8Z 7X8, Canada

ABSTRACT: Aβ peptides can assemble into amyloid fibrils, which represent one of the hallmarks of Alzheimer's disease. Recent studies, however, have focused on the behavior of small soluble Aβ oligomers that possess a much greater neurotoxicity than mature fibrils. The structural characterization of these oligomers remains difficult because of their highly dynamic and polymorphic nature. This work explores the behavior of Aβ(1−40) in a slightly basic solution (pH 9.3) at a low salt concentration (10 mM ammonium acetate). These conditions lead to the formation of small oligomers, without any signs of fibrillation for several hours. The structure and dynamics of these oligomers were characterized by circular dichroism spectroscopy, size exclusion chromatography, and millisecond time-resolved hydrogen exchange mass spectrometry (MS). Our results reveal rapid interconversion between Aβ(1−40) oligomers and monomers. The mole fraction of monomeric molecules is on the order of 40%. Oligomers consist of ∼4 Aβ(1−40) molecules on average, and the resulting assemblies have a predominantly β-sheet secondary structure. Hydrogen exchange proceeds in the EX1 regime. This feature allows the application of conformer-specific top-down MS. Electron capture dissociation is used for interrogating the deuteration behavior of the Aβ(1−40) oligomers. This approach provides a spatial resolution of ∼2 residues. The backbone amide deuteration pattern uncovered in this way is consistent with a β−turn−β motif for L17−M35. The N-terminus is involved in hydrogen bonding, as well, whereas protection gradually tapers off for C-terminal residues 35−40. Our data are consistent with earlier proposals, according to which Aβ(1−40) oligomers adopt a β-barrel structure. In general terms, this study demonstrates how top-down MS with precursor ion selection can be employed for structural studies of specific protein conformers within a heterogeneous mix.

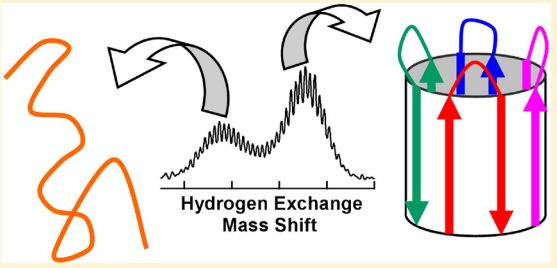

Many neurodegenerative disorders are closely linked to protein misfolding and aggregation.[1] In the case of Alzheimer's disease, the aggregation of Aβ peptides has been shown to play a key role.[2−5] Monomeric Aβ(1−40) and Aβ(1−42) are formed by γ-cleavage of the amyloid precursor protein.[6] These Aβ peptides exhibit a high propensity to self-assemble into amyloid fibrils, characterized by β-strands that run perpendicular to the fibril axis.[7] Fibril models[8−10] suggest that individual peptides are arranged in a β−turn−β motif. The 10−20 N-terminal residues appear to be disordered, followed by ∼10 residues that form the first β-strand. The turn is located in the range of residues 25−30, and it is followed by the second β-strand. Intermolecular hydrogen bonding leads to parallel stacking of the strands from individual protomers, such that two extended β-sheets are formed, one on each side of the protofibril. Several protofibrils may then be twisted around one another, resulting in mature amyloid fibrils that can exhibit different morphologies. Aβ(1−40) and Aβ(1−42) are formed in a 10:1 ratio, but the latter is more amyloidogenic and exhibits higher cytotoxicity.[4] This effect likely reflects the presence of two additional C-terminal hydrophobic residues that facilitate the formation of intermolecular contacts in Aβ(1−42).[5,11−13]

Amyloid fibrils form insoluble plaques in the brains of Alzheimer's patients. Aβ fibrils were therefore initially suspected to represent a major neurotoxic agent. More recent work, however, has demonstrated that the cytotoxicity of mature fibrils is quite low. Instead, neurodegeneration and synaptic dysfunction have been linked to small soluble Aβ oligomers.[14−20] Even dimers can impair synaptic plasticity and memory.[21,22] The mechanistic role of these soluble oligomers during the progression of Alzheimer's disease remains under investigation. There are indications that oligomers can interact with the cell surface,[23,24] possibly through specific receptors.[25]

The biophysical characterization of soluble Aβ oligomers has proven to be difficult because of their highly dynamic and polymorphic nature.[26,27] Depending on the conditions used, various heterogeneous oligomer structures that differ in their secondary, tertiary, and quaternary structure may form.[15,16,23,28−31] Large oligomers appear to exhibit a β-rich backbone arrangement resembling that seen in mature amyloid fibrils.[16,29,31−33] The situation is less clear for smaller assemblies that consist of only a few molecules.[15] Gaining more detailed insights into the properties of these small soluble Aβ oligomers may aid in the development of therapeutic strategies, such as oligomer sequestration[27] or

Received: February 14, 2012
Revised: April 7, 2012
Published: April 9, 2012

   dx.doi.org/10.1021/bi3002049 | *Biochemistry* 2012, 51, 3694−3703

disruption of intermolecular contacts by low-molecular mass compounds.[34]

Mass spectrometry (MS) continues to play a key role in deciphering many aspects related to aggregation phenomena of Aβ and other proteins.[4,35,36] Native electrospray ionization MS (ESI-MS) sometimes allows the direct detection of oligomerization intermediates.[37] Ion mobility spectrometry can yield information regarding the shape and subunit stoichiometry of these assemblies.[28,38,39] Of particular interest is the application of solution-phase hydrogen exchange MS (HX-MS), which reports on the extent of backbone amide NH protection. HX can be conducted under exchange-in conditions (labeling of a fully protiated species in D_2O) or under exchange-out conditions (labeling of a fully deuterated species in H_2O). Regions with stable hydrogen-bonded secondary structure undergo slower exchange than disordered segments.[40−45] In the simplest case, HX-MS can be applied to acquire information at the intact protein level.[46,47] More detailed insights are obtained when proteins are subjected to proteolytic digestion after isotope labeling. This approach yields spatially resolved HX data from the mass shifts of individual peptides. Unfortunately, application of this proteolysis approach to Aβ assemblies is complicated by the relatively poor digestion efficiency of Aβ, which results in limited spatial resolution.[48,49]

Gas-phase dissociation techniques have recently emerged as an alternative approach for interrogating the solution-phase HX behavior of proteins.[50] Under properly controlled conditions, both electron capture dissociation (ECD)[51] and electron transfer dissociation (ETD)[52] can preserve the backbone deuteration pattern during fragmentation, thereby eliminating scrambling artifacts.[53,54] Potential advantages of these electron-based techniques include an improved spatial resolution and the opportunity to minimize back exchange.[55] One strategy is the incorporation of ECD or ETD into the traditional digestion HX workflow, such that proteolytic peptides are broken down into smaller fragments.[56−58] Alternatively, one can bypass proteolytic digestion and instead dissociate electrosprayed protein ions after solution-phase HX.[59,60] This "top-down" approach offers the unique opportunity to select precursor ion populations with specific deuteration properties, such that the analyses can be conducted in a conformer-specific fashion.[32,61]

In an earlier study,[32] we used top-down ECD HX-MS for probing the properties of relatively large Aβ(1−42) oligomers consisting of 25−100 protomers. The resulting data were consistent with a β−turn−β backbone arrangement, reminiscent of the secondary structure seen in mature amyloid fibrils. The Aβ(1−42) oligomers of that previous work[32] were generated by incubation in F12 medium.[25,30] Keeping in mind the known dependence of the Aβ oligomer morphology on the environment,[15,16,23,28−31] we find it is interesting to determine if other solvent conditions result in different backbone HX protection patterns. Of particular interest are the properties of Aβ dimers, trimers, and tetramers, as this range encompasses the minimal size that still shows neurotoxic behavior.[21,22]

Here we explore the properties of very small soluble oligomers, formed by incubation of Aβ(1−40) under mildly basic conditions. It is shown that these assemblies adopt a predominantly tetrameric quaternary structure and that they undergo rapid equilibration with monomers. Top-down ECD data are consistent with a β−turn−β arrangement; however, the details of the isotope labeling pattern are quite different from those of large Aβ(1−42) aggregates.[32] In agreement with earlier proposals in the literature, we suggest that the Aβ(1−40) tetramer structure could represent a β-barrel.

EXPERIMENTAL PROCEDURES

Materials. Human Aβ(1−40) [DAEFRHDSGYEVHHQKLVFFAEDVGSNKGAIIGLMVGGVV (calculated molecular mass of 4329.86 Da)] was obtained from AnaSpec (San Jose, CA). HFIP, ammonium acetate, ammonium hydroxide, DMSO, blue dextrin, BSA, BLG, CA, and Ub were obtained from Sigma (St. Louis, MO). Deuterium oxide and ammonium deuteroxide were purchased from Cambridge Isotope Laboratories (Andover, MA). pH and pD values are reported as read, without correction for isotope effects.

Sample Preparation. Lyophilized Aβ(1−40) powder was dissolved in cold HFIP at a concentration of 1 mM in a microcentrifuge tube and incubated at room temperature for 1 h to establish a monomeric structure.[62] HFIP was removed by evaporation, and subsequently, the resulting clear peptide film was dissolved in anhydrous DMSO at a concentration of 5 mM. To prepare the fully deuterated peptide, Aβ(1−40) in DMSO was then diluted to 2.5 mM in D_2O at pD 11.0 (adjusted by ammonium deuteroxide), followed by incubation for 1 h at room temperature. The deuteration level of the resulting peptide was determined to be >99% by ESI-MS using direct infusion. Fully deuterated Aβ(1−40) was then diluted to 100 μM in D_2O containing 10 mM ammonium acetate (pD 9.3) at room temperature. Samples prepared in this way were analyzed within 2 h. During this time interval, there was no evidence of the formation of large aggregates or amyloid fibrils, as verified by SEC (see below). CD spectra were recorded on a Jasco (Easton, MD) J-810 spectropolarimeter using a 0.1 mm path length cuvette.

Size-Exclusion Chromatography (SEC). SEC was performed on a Waters Acquity UPLC system with a Superdex 75 10/300 GL column (GE Healthcare).[32] Aqueous ammonium acetate (10 mM, pH 9.3) was used as the mobile phase at a flow rate of 0.5 mL/min. Following the manufacturer's recommendation, the SEC column was calibrated with four standard proteins, BSA (67 kDa), BLG dimer (36.6 kDa), CA (29 kDa), and Ub (8.6 kDa). The void volume was established with blue dextran (~2 MDa). Elution profiles were recorded using a UV absorbance detector at 280 nm.

Deuterium−Hydrogen Exchange. Isotope labeling was conducted under exchange-out conditions,[63] i.e., fully deuterated Aβ(1−40) labeled in H_2O. We will refer to this scenario as "DHX", to distinguish it from the reverse (exchange-in, HDX) scenario. Our experiments were conducted using a previously described[55] two-stage continuous-flow mixing device that was coupled online to the ion source of the mass spectrometer. The first mixing step initiates DHX by exposing Aβ(1−40) to the labeling solution (10 mM ammonium acetate in H_2O at pH 9.3). In the second step, the solution is mixed with 0.4% formic acid in acetonitrile. This second mixing step serves several purposes. (i) Isotope labeling is quenched under acidic conditions after a predetermined DHX time interval (ranging from 50 ms to 8 s, as determined by the length of the labeling capillary). (ii) The highly denaturing conditions after the second mixing step ensure dissociation of the oligomer into monomers. As a result, for the readout of DHX experiments, all Aβ(1−40) molecules are observed in their monomeric form, regardless of the oligomerization state in bulk solution and during labeling.[32] (iii) The presence of acid in combination with an organic makeup solvent dramatically enhances the signal intensity during online ESI-MS.[64] The flow rates of deuterated

dx.doi.org/10.1021/bi3002049 | Biochemistry 2012, 51, 3694−3703

Aβ(1−40), labeling solution, and quenching solution were 4, 16, and 20 μL/min, respectively. The outlet of the second mixer was coupled directly to the ESI stainless steel capillary (length of 9 cm, inside diameter of 100 μm), resulting in a time interval of ∼1 s between quenching and ESI. Solution-phase isotope back exchange is negligible under these conditions.[55]

Mass Spectrometry and Top-Down ECD. DHX experiments with intact Aβ(1−40) were conducted using an ESI Q-TOF instrument (Waters, Manchester, U.K.), with a source temperature of 80 °C, a desolvation temperature of 120 °C, and a cone voltage of 45 V. Top-down ECD data were acquired on a 12 T Apex-Qe hybrid FTMS instrument (Bruker Daltonics, Billerica, MA) using parameter settings described previously.[55] Approximately 1800 scans were accumulated over the m/z range of 250−2500 for each ECD spectrum within 30 min. ECD spectra were acquired after solution-phase DHX for 50 ms from front-end quadrupole-isolated $[M + 5H]^{5+}$ ions of Aβ(1−40), with an isolation window centered at m/z 875. As discussed in more detail below, this approach allows the selective structural interrogation of oligomeric Aβ(1−40).[32] FTMS calibration was performed with intact ions and ECD fragments of ubiquitin. Neutral Aβ(1−40) contains 66 exchangeable hydrogens. Of these, 39 are amide backbone hydrogens, 24 are on side chains, and three are on the termini; 32 c ions and 22 $z^{\bullet}$ ions were detected after ECD of unlabeled Aβ(1−40), representing cleavage of 33 of 39 amide bonds. Because of signal-to-noise degradation caused by expansion of the isotope envelope after DHX,[65] only a subset of these ions could be considered for data analysis: c_3−c_7, c_{10}, c_{13}−c_{15}, c_{19}, c_{21}, c_{22}, c_{24}−c_{27}, c_{34}, c_{35}, and c_{37}. Data for intact Aβ(1−40) were used in lieu of c_{39}. Control experiments with nondeuterated Aβ(1−40) confirmed the absence of $c^{\bullet}$ or z ions[66] under the conditions used here.

Analysis of DHX Data. Spatially resolved deuteration information was obtained from top-down ECD data following a strategy similar to that described previously,[55] with some modifications. Briefly, the number of backbone amide deuterium atoms retained in a c ion after DHX can be expressed as[67]

$$N_{\text{amide deuterium}} = N_{\text{total deuterium}} - N_{\text{non-amide deuterium}} \quad (1)$$

where $N_{\text{total deuterium}}$ is the total number of deuterium atoms in the fragment ion, excluding charge carriers, and $N_{\text{nonamide deuterium}}$ is the number of deuterium atoms in side chains and termini for each of the c ions.[68,69] $N_{\text{non-amide deuterium}}$ can be determined as (number of non-amide exchangeable sites) × P, where P is the deuteration level of a bradykinin internal standard.[55] For the experiments discussed below, P was found to be 24.5%, slightly above the expected value of 20%. This difference may reflect small deviations between nominal and actual flow rates of the mixing device. $N_{\text{total deuterium}}$ can be determined as

$$N_{\text{total deuterium}} = \frac{n(R - R_0)}{m_D - m_H} - nP \quad (2)$$

where n is the charge state of the ion, m_D (2.0141 amu) is the atomic mass of deuterium, m_H (1.0078 amu) is the mass of hydrogen, R is the centroid m/z value of the c ion after DHX, and R_0 is the corresponding centroid m/z value for the unlabeled ion. The amide deuteration level D' of residue 2 (the first backbone amide in the chain) is then given by

$$D'_2 = N_{\text{amide deuterium}}(c_1) \quad (3)$$

and for subsequent fragment ions the deuteration level D'_q of backbone amide site q can be calculated as

$$D'_q = N_{\text{amide deuterium}}(c_{q-1}) - N_{\text{amide deuterium}}(c_{q-2}) \quad (4)$$

In cases where ions are missing from the consecutive ion series, average D' values were assigned to each of the intervening amide groups.[55] As determined by the isotopic makeup of the labeling solution, the D' values obtained in this way cover the range between 0.245 and 1.0. To simplify the subsequent discussion, these values were normalized according to eq 5.[42] Error bars are based on duplicate independent experiments.[70]

$$D = \frac{D' - 0.245}{1 - 0.245} \quad (5)$$

RESULTS AND DISCUSSION

Size Exclusion Chromatography and Circular Dichroism Spectroscopy. Incubation of Aβ(1−40) in 10 mM ammonium acetate (pH 9.3) results in SEC retention behavior that corresponds to an average molecular mass ($\bar{M}_{\text{SEC}}$) of 11 kDa (Figure 1). This value is 2.6 times larger than the molecular mass of 4.3 kDa of monomeric Aβ(1−40). The SEC data, therefore, indicate the formation of small soluble aggregates under the conditions used here. Close inspection reveals that the Aβ(1−40)

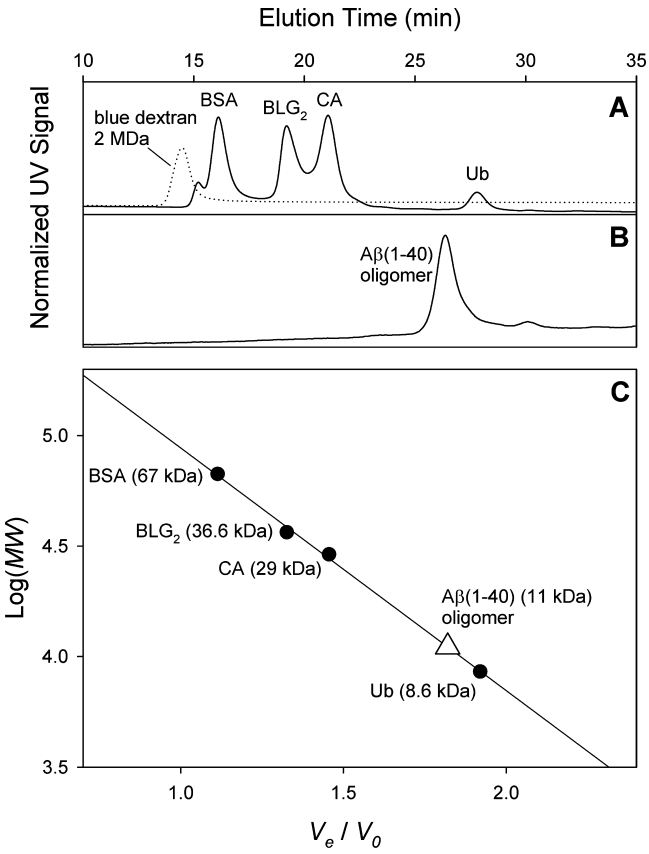

Figure 1. SEC analysis of Aβ(1−40) in 10 mM ammonium acetate (pH 9.3). (A) Elution profile of calibrants. (B) Elution profile of Aβ(1−40), obtained under the same conditions used for panel A. The small signal at 30 min (∼6.3 kDa) likely represents an impurity. (C) Linear regression analysis used for determining the average molecular mass of Aβ(1−40). The x-axis represents V_e/V_0, where V_e and V_0 are the elution volumes of the various protein species and the blue dextran standard, respectively.

dx.doi.org/10.1021/bi3002049 | Biochemistry 2012, 51, 3694−3703

peak width (fwhm) is ~1.7-fold greater than those of the globular standard proteins, suggesting considerable heterogeneity in the Aβ(1−40) oligomerization state. This interpretation is supported by the DHX data discussed below, which indicate that Aβ(1−40) oligomers are in rapid equilibrium with monomers.

The Aβ(1−40) samples exhibit a CD spectrum with a minimum at around 209 nm (Figure 2). Minima in this range

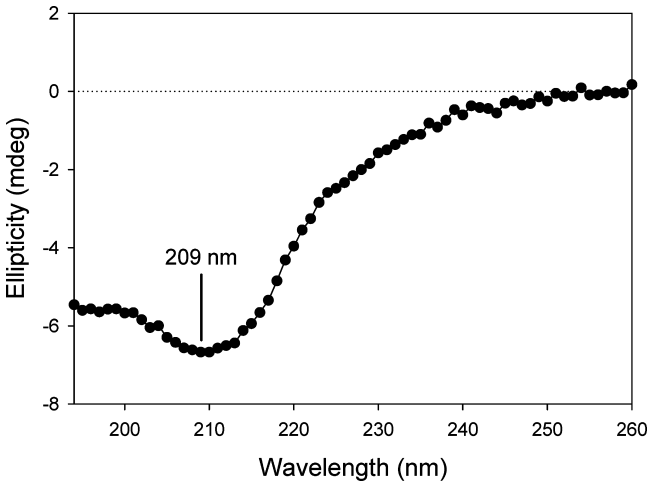

Figure 2. CD spectrum of 100 μM Aβ(1−40) in aqueous solution containing 10 mM ammonium acetate (pH 9.3).

have previously been reported for cross-linked Aβ(1−40) dimers, trimers, and tetramers.[15] Monomeric Aβ(1−40) is known to adopt a disordered structure, with an ellipticity minimum at 200 nm.[15,71] In contrast, mature amyloid fibrils with their highly ordered β-sheet rich secondary structure show a minimum at 216 nm.[15] The minimum at 209 nm observed here reveals that our samples possess partial β-strand character, with an overall degree of structural organization between those of monomers and fibrils. At the same time, however, the relatively flat region seen in Figure 2 around 200 nm suggests the additional presence of extensively disordered species [likely monomers (see below)].[15] The weakly negative ellipticity in the 222 nm range implies that the samples studied here form little, if any, helical structure.

Aβ(1−40) Structural Dynamics Probed by DHX. Millisecond time-resolved DHX-MS results in bimodal mass distributions (Figure 3). With an increasing labeling time, the high-mass contribution decreases in intensity, whereas the low-mass signal increases in intensity. This phenomenon represents the hallmark of the EX1 regime, implying the cooperative interconversion between unprotected conformers (low-mass envelope) and species that are significantly protected (high-mass envelope).[72,73] The peak maximum in Figure 3E (t = 8 s) is located at m/z 870.8, close to the value of m/z 870.5 that is expected for fully labeled Aβ(1−40). The behavior of this low-mass envelope is consistent with the presence of monomeric Aβ(1−40).[46] In contrast, the high-mass envelope is ascribed to the presence of Aβ(1−40) oligomers that exhibit DHX protection because of intermolecular and/or intramolecular hydrogen bonding.

The interpretation of our DHX data in terms of an oligomer−monomer equilibrium is supported by SEC peak broadening (Figure 1) and by the observation of both ordered and disordered elements in the CD spectrum of Figure 2. In addition, EX1 data

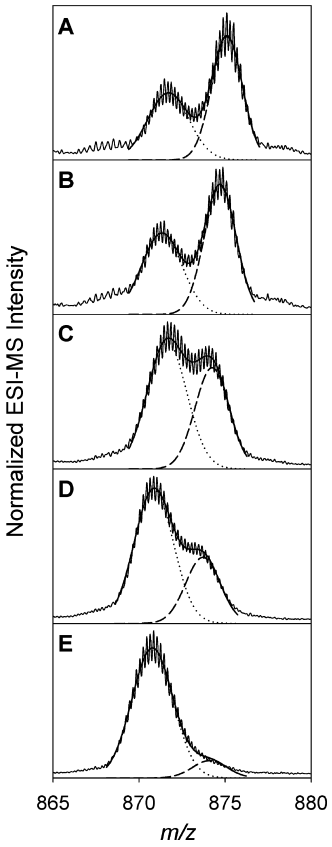

Figure 3. Mass distribution of Aβ(1−40) after isotope labeling, using DHX times of 50 ms (A), 100 ms (B), 500 ms (C), 1 s (D), and 8 s (E). The data refer to the +5 charge state. Note that the experimental conditions were chosen to ensure oligomer dissociation prior to ESI-MS detection. Also shown are Gaussian decompositions that provide estimates of the high- and low-mass contributions for the various DHX times.

qualitatively similar to those of Figure 3 have recently been reported for binding equilibria involving mature amyloid fibrils and their monomeric building blocks.[46,70] It is noteworthy, however, that the EX1 process in Figure 3 goes to completion within seconds, whereas isotope exchange for amyloid fibrils takes place on the order of days or weeks.[46,70] Thus, aggregate−monomer equilibration occurs many orders of magnitude faster for small Aβ(1−40) oligomers than for amyloid fibrils. Close inspection of Figure 3 also reveals the occurrence of slight gradual shifts in the peak maxima of the DHX mass distributions, resulting from subglobal (EX2) structural dynamics. Combined EX1−EX2 processes of this type have previously been reported for other proteins.[63,72,73]

Additional insights into the nature of the Aβ(1−40) oligomer−monomer equilibrium can be obtained by analyzing the EX1 dynamics of Figure 3 in more detail. Gaussian decomposition yields the relative fraction of the high-mass component as a function of time (Figure 4). For DHX times up to 1 s, the resulting kinetics are described well by a single-exponential fit with an apparent rate constant k_{op} of 0.7 s^{-1} (solid line in Figure 4). Because exchange occurs under EX1 conditions, this "opening" rate constant reflects the kinetics of the oligomer → monomer dissociation step.[74] Extrapolation of the DHX kinetics to time zero reveals a burst-phase amplitude (a) of 0.60. From this, we can conclude that 60% of the Aβ(1−40) molecules are bound in the oligomeric state, whereas the remainder (40%) is monomeric.

dx.doi.org/10.1021/bi3002049 | *Biochemistry* 2012, 51, 3694−3703

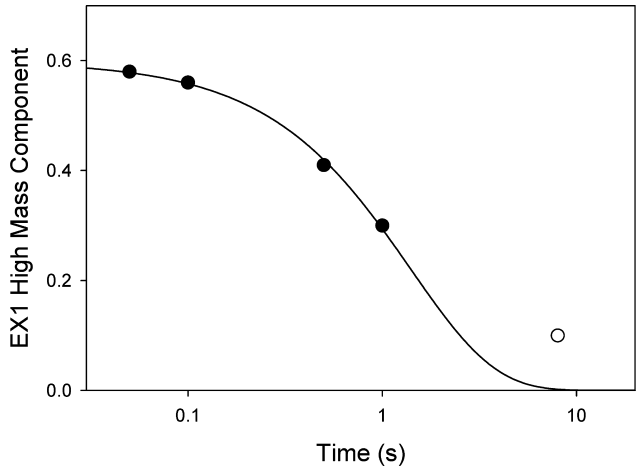

Figure 4. EX1 kinetics, reflecting the relative contribution of the high-mass component in Figure 3. Individual data points were determined as (high-mass peak area)/(high-mass peak area + low-mass peak area). Peak areas were determined from the Gaussian decompositions of Figure 3. The solid line is an exponential fit with $f = a \exp(-k_{op}t)$, where t is the DHX time, $a = 0.60$, and $k_{op} = 0.7\ s^{-1}$. The data point for 8 s was not considered in the fitting procedure because it deviates from single-exponential behavior, possibly because of structural heterogeneity and/or the presence of parallel dissociation equilibria.

Characterizing the Aβ(1−40) Oligomer Binding Stoichiometry. On the basis of the assertion that the Aβ(1−40) samples represent an oligomer/monomer mixture, we can estimate the number n that describes the binding stoichiometry of the $A\beta(1-40)_n$ oligomers. We make the simplifying assumption that the oligomer size can be approximated by a single value of n. The SEC data of Figure 1 yield a mass-average (as opposed to a number-average) molecular mass that is given by

$$\bar{M}_{SEC} = \frac{C_M M_M^2 + C_O M_O^2}{C_M M_M + C_O M_O} \quad (6)$$

where C_M, C_O, M_M, and M_O refer to the solution-phase concentrations and molecular masses of monomeric and oligomeric Aβ(1−40), respectively. From the DHX kinetic information (Figure 4), we know that $C_M = 0.4k$ and $C_O = k(0.6/n)$, where k is a conversion factor that will cancel out in the next step. When $M_O = nM_M$, eq 6 simplifies to

$$11\ \text{kDa} = 4.3\ \text{kDa}(0.4 + 0.6 \times n) \quad (7)$$

from which the value of n is found to be 3.6. Thus, we conclude that the oligomers most likely consist of four Aβ(1−40) molecules on average. This estimate is consistent with recent single-molecule fluorescence investigations[27] and cross-linking experiments[15] that were performed with Aβ(1−40) oligomers using solution conditions slightly different from those employed here.

We also attempted to characterize the Aβ(1−40) aggregation state by native ESI-MS. Various oligomerization states all the way up to 16-mers can be detected by this approach at pH 7.4.[39] Unfortunately, under the conditions used here (pH 9.3), where the Aβ oligomerization propensity is reduced, this approach proved to be unsuccessful. The resulting spectra (not shown) were dominated by Aβ(1−40) monomeric ions, supporting the view that the solution-phase binding equilibrium involves monomeric Aβ(1−40). However, only trace amounts of larger species were observed. It thus appears that Aβ(1−40) oligomers exhibit an exceedingly low ionization efficiency under the conditions used here, pointing to conformation-dependent ion suppression.[75,76] Alternatively, Aβ(1−40) assemblies might undergo disruption during ESI.

Spatially Resolved Backbone Amide Deuteration of Aβ(1−40) Oligomers. For uncovering the degree of protection at individual NH backbone sites in Aβ(1−40) oligomers, the high-mass portion of the DHX envelope at 50 ms (Figure 3A) was subjected to top-down ECD. This approach yields conformer-specific data; i.e., the oligomer DHX behavior can be uncovered without interference from monomeric Aβ(1−40) that coexists in solution during labeling.[32] ECD resulted in 19 c ions with adequate signal-to-noise ratios for reliable analyses of their DHX mass shifts (Figures 5 and 6). The average spatial resolution obtained in this way corresponds to ∼2 residues, which is a significant improvement over earlier proteolytic digestion data.[48,49]

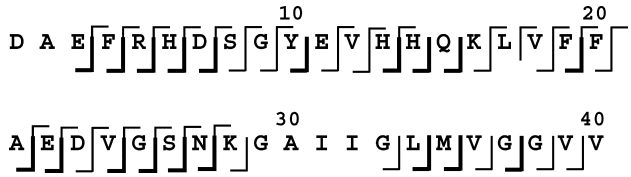

Figure 5. Sequence of Aβ(1−40), with ECD cleavage sites (c and z• ions[66]) that were detected under the conditions used in this work. Only cleavage sites indicated with bold lines provided fragment ion signals with signal-to-noise ratios that were adequate for DHX analyses.

From the mass shifts of these ECD fragments, it is possible to determine the number of backbone amide deuterium atoms retained in each of the c ions (Figure 7). In the hypothetical case of totally unprotected Aβ(1−40), all ND sites would undergo DHX with a half-life of roughly 1 ms under the slightly basic conditions used here.[77] This scenario is indicated as a dashed line in Figure 7. Also included in Figure 7 is the situation that would expected for complete protection. The experimental data measured for a labeling time of 50 ms fall between these two limiting scenarios (Figure 7).

Transformation of the data in Figure 7 using eqs 2−5 yields the deuteration level D for the amide groups along the backbone of Aβ(1−40) oligomers (Figure 8). With the normalization procedure used here (eq 5), amides that are completely protected will be characterized by a D of 1. Conversely, sites that are totally unprotected have a D of 0. Fractional D values reflect partial protection, caused either by marginal structural stability or by conformational heterogeneity. To interpret the data of Figure 8, we rely on the tenet that the deuteration behavior primarily reflects the extent of hydrogen bonding, rather than solvent accessibility.[78]

Figure 8 reveals relatively high D values for the N-terminal half of the backbone, ranging between 0.6 and almost 1. The highest protection in this range is observed for D1−E3, as well as L17−E22. Protection decreases to <0.6 for D23−G25. S26 and K28 show almost no protection. Interestingly, the intervening N27 remains almost completely deuterated. Residues G29−M35 are characterized by D values of ∼0.75. Protection gradually tapers off to ≈0.4 for the five C-terminal residues.

Implications for the Structure of Aβ(1−40) Oligomers. Our DHX data do not provide direct information regarding the structural arrangement of individual polypeptide chains in

dx.doi.org/10.1021/bi3002049 | Biochemistry 2012, 51, 3694−3703

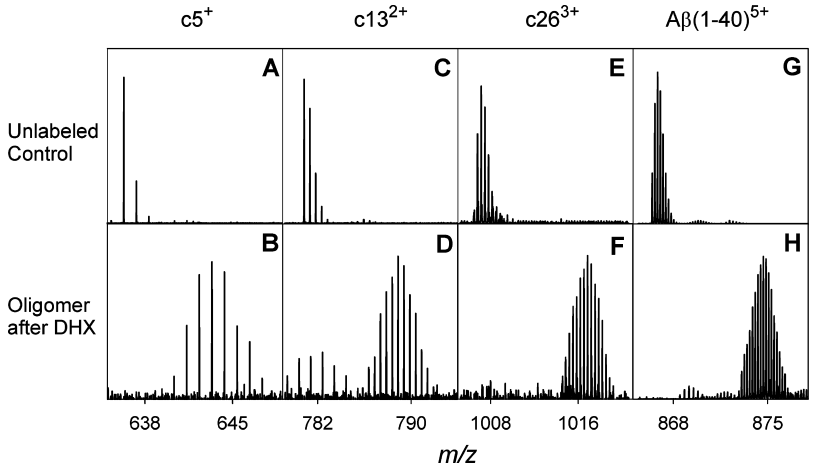

Figure 6. Selected ion signals, obtained by subjecting the +5 charge state of Aβ(1−40) to ECD. The top row shows data for the nondeuterated control; the bottom row shows data after precursor ion selection of the high-mass envelope for a DHX time of 50 ms (corresponding to oligomer, m/z 875 in Figure 3A). Data are shown for three different fragment ions and intact Aβ(1−40).

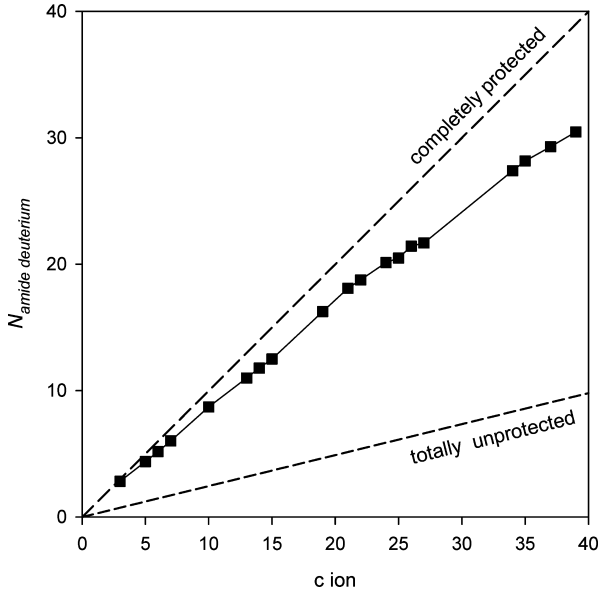

Figure 7. Number of amide deuterium atoms ($N_{\text{amide deuterium}}$, eq 1) retained in various ECD fragment ions of Aβ(1−40) after DHX for 50 ms. Also shown (−−−) are the two hypothetical scenarios in which all of the amide groups are completely protected and in which they are devoid of protection.

Aβ(1−40) oligomers. It is nonetheless instructive to discuss a few pertinent points. Earlier work has suggested that the backbone arrangement of Aβ oligomers could resemble the β−turn−β secondary structure of mature amyloid fibrils.[16,29,31,32] It is interesting to consider this possibility for the Aβ(1−40) oligomers of this work. Partial β-sheet content is readily apparent from the CD data of Figure 2. In the deuteration map of Figure 8, the corresponding β-strands should appear as contiguous regions that are highly protected and quite hydrophobic.[79] On the basis of these criteria, L17−E22 and G29−M35 represent likely β-strand regions. The intervening residues include S26 and K28, which are unprotected, while N27 remains almost completely deuterated. This pattern is consistent with a turn in the range of residues 26−28. Turns are often stabilized by a single hydrogen-bonded N−H(D) group,[80] which is in line with the high D value seen for N27. Overall, our oligomer deuteration data are therefore consistent with a β−turn−β backbone arrangement for residues L17−M35 (Figure 9A). The locations proposed for the turn and for the two β-strands roughly match the sequence region where this motif is located in amyloid fibrils.[8−10]

Not all features of the measured oligomer deuteration pattern, however, are consistent with a fibril-like secondary structure. Oligomers show significant protection throughout the N-terminus, especially for residues 1−11 (Figure 8). This

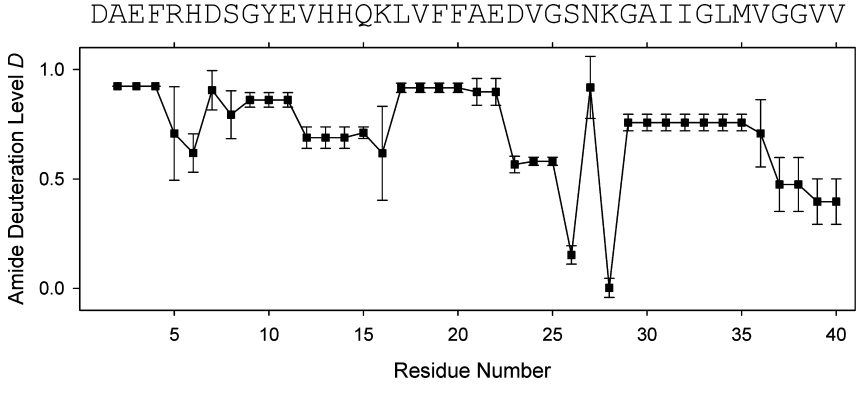

Figure 8. Backbone deuteration level D for individual amide linkages in Aβ(1−40) oligomers after DHX for 50 ms. The data were obtained by analyzing mass shifts of ECD fragment ions after isotope labeling of Aβ(1−40) in solution, using eqs 1−5.

dx.doi.org/10.1021/bi3002049 | Biochemistry 2012, 51, 3694−3703

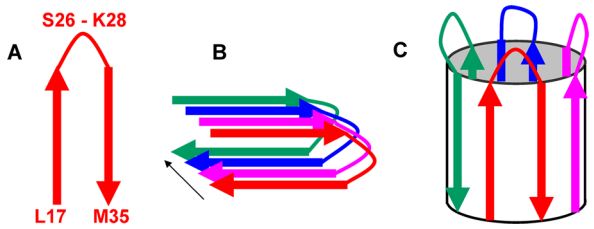

Figure 9. (A) Schematic representation of the proposed β–loop–β secondary structure for individual Aβ(1–40) molecules within an oligomeric assembly. Residues 1–16 and 36–40 have been omitted. (B) Cartoon representation of an Aβ(1–40) tetramer, where individual protomers are stacked in a fibril-like fashion. (C) Cartoon representation of a β-barrel tetramer arrangement (a scenario more likely than that in panel B, as discussed in the text). Note that all details such as the tilt angle of individual strands in panel C have been omitted.

region must therefore be involved in hydrogen bonding, as well. A similar behavior was recently reported for much larger Aβ(1–40)[33] and Aβ(1–42)[32] oligomers. In contrast, amyloid fibrils exhibit a highly disordered N-terminus.[8–10] Another notable feature is the gradually decreasing protection seen for the five C-terminal residues in Figure 8. This attribute is different from the situation in fibrils and larger oligomers,[32,33] where the C-terminal end of the backbone forms a tightly hydrogen-bonded β-strand all the way to the last residue.[8,9]

The SEC data of this work suggest that the oligomers studied here consist of ~4 Aβ(1–40) molecules. It is interesting to speculate how the four protomers might be joined together, subject to the restriction that their backbone must involve a β–turn–β arrangement. Two possibilities will be considered. (i) One might suggest that the four Aβ(1–40) protomers are stacked in a fibril-like fashion,[8–10] stabilized by interchain hydrogen bonding. This arrangement would lead to two parallel β-sheets, each one consisting of four strands (Figure 9B). In our view, such an Aβ(1–40)$_4$ structure seems unlikely because of the large fraction of unsaturated backbone hydrogen bond donor–acceptor sites in the first and the fourth protomers (red and green in Figure 9B). In addition, spectroscopic data strongly suggest an antiparallel β-sheet structure for Aβ(1–40) oligomers,[23] which is incompatible with a stacked fibril-like arrangement (Figure 9B). (ii) Alternatively, each β–turn–β element could fold into a two-stranded antiparallel sheet. Four of these hairpins could then loop around to form a β-barrel that is stabilized by both intermolecular and intramolecular hydrogen bonds (Figure 9C). Support for such antiparallel β-barrel models comes not only from vibrational spectroscopy[23] but also from computational modeling[31] and X-ray data for related systems.[81] In the absence of high-resolution structural information, the proposal of Aβ(1–40)$_4$ as an antiparallel β-barrel therefore represents a reasonable working hypothesis (Figure 9C). The cartoon of Figure 9C does not make any assertions regarding residues 1–16, which are also hydrogen bonded (according to the data of Figure 8). Helix formation in this region could represent one option,[31,82] but this possibility is not strongly supported by the CD data of Figure 2.

■ CONCLUSIONS

This work demonstrates that incubation of Aβ(1–40) at pH 9.3 in 10 mM ammonium acetate leads to the formation of small soluble oligomers that are in rapid equilibrium with monomeric species. The oligomers formed under these conditions have an average size in the tetramer range, with a predominantly β-sheet secondary structure. Similar characteristics have previously been reported for Aβ oligomers formed under other conditions.[15,16,23,27–31,33] As noted in the introductory section, structural characterization of those other assemblies has been frustrated by their heterogeneous and highly dynamic nature. Also, the Aβ oligomerization behavior is highly dependent on the experimental conditions.[26,27] The significance of the conditions used here lies in the fact that solvent used is amenable to online ESI-MS. As a result, isotope labeling experiments can be conducted without any chromatographic steps that would interfere with the solution-phase DHX pattern. More importantly, the slightly basic pH provides EX1 conditions with two isotope envelopes that are clearly separated for short labeling times. This feature allows a selective interrogation of the oligomer amide protection pattern.

Analysis of our DHX data suggests that residues L17–M35 in Aβ(1–40) oligomers adopt a β–turn–β backbone arrangement. By combining the data of this work with previous reports in the literature, we suggest that the oligomers considered here consist of four Aβ(1–40) molecules that may assemble into an antiparallel β-barrel (Figure 9). This proposal is supported by recent data on other amyloidogenic species.[81] One possible mechanism whereby β-barrels could mediate neurotoxicity is insertion into the cell membrane.[23] It remains to be established how much the oligomers formed under the conditions of this work resemble assemblies that are found in the brains of Alzheimer's patients.[14–20,22]

In general terms, our study highlights how the application of a newly developed biophysical tool (DHX with conformer-specific top-down ECD)[32] can aid in the characterization of heterogeneous protein systems that encompass coexisting conformations or binding states. In the future, it should become possible to use such isotope exchange data as constraints for computer simulations, ultimately resulting in high-resolution structural models that can be subjected to further experimental validation.[83]

■ AUTHOR INFORMATION

Corresponding Author

*Telephone: (519) 661-2111, ext. 86313. Fax: (519) 661-3022. E-mail: konerman@uwo.ca.

Funding

This work was supported by the Natural Sciences and Engineering Council of Canada, Genome Canada, Genome BC, PrioNet Canada, and the Canada Research Chairs Program.

Notes

The authors declare no competing financial interest.

■ ACKNOWLEDGMENTS

CD experiments were conducted at the University of Western Ontario Biomolecular Interactions and Conformations Facility.

■ ABBREVIATIONS

Aβ, amyloid β-peptide; APP, amyloid precursor protein; BLG, β-lactoglobulin; BSA, bovine serum albumin; CA, carbonic anhydrase; CD, circular dichroism; DHX, deuterium–hydrogen exchange; DMSO, dimethyl sulfoxide; ECD, electron capture dissociation; ESI, electrospray ionization; ETD, electron transfer dissociation; FTMS, Fourier transform mass spectrometer; HX, hydrogen exchange; HFIP, hexafluoro-2-propanol; MS, mass spectrometry; SEC, size exclusion chromatography; Ub, ubiquitin.

REFERENCES

(1) Chiti, F., and Dobson, C. M. (2006) Protein Misfolding, Functional Amyloid, and Human Disease. *Annu. Rev. Biochem. 75*, 333−366.

(2) Schnabel, J. (2011) Amyloid: Little Proteins, Big Clues. *Nature 475*, S12−S14.

(3) Hardy, J., and Selkoe, D. J. (2002) The Amyloid Hypothesis of Alzheimer's Disease: Progress and Problems on the Road to Therapeutics. *Science 297*, 353−356.

(4) Teplow, D. B., Lazo, N. D., Bitan, G., Bernstein, S., Wyttenbach, T., Bowers, M. T., Baumketner, A., Shea, J. E., Urbanc, B., Cruz, L., Borreguero, J., and Stanley, H. E. (2006) Elucidating amyloid β-protein folding and assembly: A multidisciplinary approach. *Acc. Chem. Res. 39*, 635−645.

(5) Detoma, A. S., Salamekh, S., Ramamoorthy, A., and Lim, M. H. (2012) Misfolded proteins in Alzheimer's disease and type II diabetes. *Chem. Soc. Rev. 41*, 608−621.

(6) St. George-Hyslop, P., and Schmitt-Ulms, G. (2010) Alzheimer's disease: Modulating γ-secretase. *Nature 467*, 36−37.

(7) Hellstrand, E., Boland, B., Walsh, D. M., and Linse, S. (2010) Amyloid β-Protein Aggregation Produces Highly Reproducible Kinetic Data and Occurs by a Two-Phase Process. *ACS Chem. Neurosci. 1*, 13−18.

(8) Petkova, A. T., Ishii, Y., Balbach, J. J., Antzutkin, O. N., Leapman, R. D., Delaglio, F., and Tycko, R. (2002) A structural model for Alzheimer's β-amyloid fibrils based on experimental constraints from solid state NMR. *Proc. Natl. Acad. Sci. U.S.A. 99*, 16742−16747.

(9) Paravastu, A. K., Leapman, R. D., Yau, W. M., and Tycko, R. (2008) Molecular structural basis for polymorphism in Alzheimer's β-amyloid fibrils. *Proc. Natl. Acad. Sci. U.S.A. 105*, 18349−18354.

(10) Lührs, T., Ritter, C., Adrian, M., Riek-Loher, D., Bohrmann, B., Dobeli, H., Schubert, D., and Riek, R. (2005) 3D structure of Alzheimer's amyloid-β(1−42) fibrils. *Proc. Natl. Acad. Sci. U.S.A. 102*, 17342−17347.

(11) Kim, W., and Hecht, M. H. (2005) Sequence Determinants of Enhanced Amyloidogenicity of Alzheimer Aβ42 Peptide Relative to Aβ40. *J. Biol. Chem. 280*, 35069−35076.

(12) Bitan, G., Kirkitadze, M. D., Lomakin, A., Vollers, S. S., Benedek, G. B., and Teplow, D. B. (2003) Amyloid β-protein (Aβ) assembly: Aβ40 and Aβ42 oligomerize through distinct pathways. *Proc. Natl. Acad. Sci. U.S.A. 100*, 330−335.

(13) Fawzi, N. L., Ying, J., Ghirlando, R., Torchiam, D. A., and Clore, G. M. (2011) Atomic-resolution dynamics on the surface of amyloid-β protofibrils probed by solution NMR. *Nature 480*, 268−272.

(14) Haass, C., and Selkoe, D. J. (2007) Soluble protein oligomers in neurodegeneration: Lessons from the Alzheimer's amyloid β-peptide. *Nat. Rev. Mol. Cell Biol. 8*, 101−112.

(15) Ono, K., Condron, M. M., and Teplow, D. B. (2009) Structure-neurotoxicity relationships of amyloid β-protein oligomers. *Proc. Natl. Acad. Sci. U.S.A. 106*, 14745−14750.

(16) Yu, L., Edalji, R., Harlan, J. E., Holzman, T. F., Lopez, A. P., Labkovsky, B., Hillen, H., Barghorn, S., Ebert, U., Richardson, P. L., Miesbauer, L., Solomon, L., Bartley, D., Walter, K., Johnson, R. W., Hajduk, P. J., and Olejniczak, E. T. (2009) Structural characterization of a soluble amyloid β-peptide oligomer. *Biochemistry 48*, 1870−1877.

(17) Huang, T. H., Yang, D. S., Plaskos, N. P., Go, S., Yip, C. M., Fraser, P. E., and Chakrabartty, A. (2000) Structural studies of soluble oligomers of the Alzheimer β-amyloid peptide. *J. Mol. Biol. 297*, 73−87.

(18) Glabe, C. G. (2008) Structural Classification of Toxic Amyloid Oligomers. *J. Biol. Chem. 283*, 29639−29643.

(19) Lesne, S., Koh, M. T., Kotilinek, L., Kayed, R., Glabe, C. G., Yang, A., Gallagher, M., and Ashe, K. H. (2006) A specific amyloid-β protein assembly in the brain impairs memory. *Nature 440*, 352−357.

(20) Koffie, R. M., Meyer-Luehmann, M., Hashimoto, T., Adams, K. W., Mielke, M. L., Garcia-Alloza, M., Micheva, K. D., Smith, S. J., Kim, M. L., Lee, V. M., Hyman, B. T., and Spires-Jones, T. L. (2009) Oligomeric amyloid β associates with postsynaptic densities and correlates with excitatory synapse loss near senile plaques. *Proc. Natl. Acad. Sci. U.S.A. 106*, 4012−4017.

(21) Jin, M., Shepardson, N., Yang, T., Chen, G., Walsh, D., and Selkoe, D. J. (2011) Soluble amyloid β-protein dimers isolated from Alzheimer cortex directly induce Tau hyperphosphorylation and neuritic degeneration. *Proc. Natl. Acad. Sci. U.S.A. 108*, 5819−5824.

(22) Shankar, G. M., Li, S., Mehta, T. H., Garcia-Munoz, A., Shepardson, N. E., Smith, I., Brett, F. M., Farrell, M. A., Rowan, M. J., Lemere, C. A., Regan, C. M., Walsh, D. M., Sabatini, B. L., and Selkoe, D. J. (2008) Amyloid-β protein dimers isolated directly from Alzheimer's brains impair synaptic plasticity and memory. *Nat. Med. 14*, 837−842.

(23) Cerf, E., Sarroukh, R., Tamamizu-Kato, S., Breydo, L., Derclaye, S., Dufrêne, Y. F., Narayanaswami, V., Goormaghtigh, E., Ruysschaert, J. M., and Raussens, V. (2009) Antiparallel β-sheet: A signature structure of the oligomeric amyloid β-peptide. *Biochem. J. 421*, 415−423.

(24) Campioni, S., Mannini, B., Zampagni, M., Pensalfini, A., Parrini, C., Evangelisti, E., Relini, A., Stefani, M., Dobson, C. M., Cecchi, C., and Chiti, F. (2010) A causative link between the structure of aberrant protein oligomers and their toxicity. *Nat. Chem. Biol. 6*, 140−147.

(25) Lauren, J., Gimbel, D. A., Nygaard, H. B., Gilbert, J. W., and Strittmatter, S. M. (2009) Cellular prion protein mediates impairment of synaptic plasticity by amyloid-β oligomers. *Nature 457*, 1128−1132.

(26) Colletier, J. P., Laganowsky, A., Landau, M., Zhao, M., Soriaga, A. B., Goldschmidt, L., Flot, D., Cascio, D., Sawaya, M. R., and Eisenberg, D. (2011) Molecular basis for amyloid-β polymorphism. *Proc. Natl. Acad. Sci. U.S.A. 108*, 16938−16943.

(27) Narayan, P., Orte, A., Clarke, R. W., Bolognesi, B., Hook, S., Ganzinger, K. A., Meehan, S., Wilson, M. R., Dobson, C. M., and Klenerman, D. (2012) The extracellular chaperone clusterin sequesters oligomeric forms of the amyloid-β(1−40) peptide. *Nat. Struct. Mol. Biol. 19*, 79−83.

(28) Bernstein, S. L., Dupuis, N. F., Lazo, N. D., Wyttenbach, T., Condron, M. M., Bitan, G., Teplow, D. B., Shea, J.-E., Ruotolo, B. T., Robinson, C. V., and Bowers, M. T. (2009) Amyloid-β protein oligomerization and the importance of tetramers and dodecamers in the aetiology of Alzheimer's disease. *Nat. Chem. 1*, 326−331.

(29) Chimon, S., Shaibat, M. A., Jones, C. R., Calero, D. C., Aizezi, B., and Ishii, Y. (2007) Evidence of fibril-like β-sheet structures in a neurotoxic amyloid intermediate of Alzheimer's β-amyloid. *Nat. Struct. Mol. Biol. 14*, 1157−1164.

(30) Chromy, B. A., Nowak, R. J., Lambert, M. P., Viola, K. L., Chang, L., Velasco, P. T., Jones, B. W., Fernandez, S. J., Lacor, P. N., Horowitz, P., Finch, C. E., Krafft, G. A., and Klein, W. L. (2003) Self-assembly of Aβ(1−42) into globular neurotoxins. *Biochemistry 42*, 12749−12760.

(31) Shafrir, Y., Durell, S. R., Anishkin, A., and Guy, H. R. (2010) β-Barrel models of soluble amyloid β oligomers and annular protofibrils. *Proteins 78*, 3458−3472.

(32) Pan, J., Han, J., Borchers, C. H., and Konermann, L. (2011) Conformer-Specific Hydrogen Exchange Analysis of Aß(1−42) Oligomers by Top-Down Electron Capture Dissociation Mass Spectrometry. *Anal. Chem. 83*, 5386−5393.

(33) Haupt, C., Leppert, J., Ronicke, R., Meinhardt, J., Yadav, J. K., Ramachandran, R., Ohlenschlager, O., Reymann, K. G., Gorlach, M., and Fändrich, M. (2012) Structural Basis of β-Amyloid Dependent Synaptic Dysfunctions. *Angew. Chem., Int. Ed. 51*, 1576−1579.

(34) Abelein, A., Bolognesi, B., Dobson, C. M., Graslund, A., and Lendel, C. (2012) Hydrophobicity and Conformational Change as Mechanistic Determinants for Nonspecific Modulators of Amyloid β Self-Assembly. *Biochemistry 51*, 126−137.

(35) Ashcroft, A. E. (2010) Mass Spectrometry and the Amyloid Problem: How Far Can We Go in the Gas Phase? *J. Am. Soc. Mass Spectrom. 21*, 1087−1096.

(36) Murray, M. M., Bernstein, S. L., Nyugen, V., Condron, M. M., Teplow, D. B., and Bowers, M. T. (2009) Amyloid β protein: Aβ40 inhibits Aβ42 oligomerization. *J. Am. Chem. Soc. 131*, 6316−6317.

(37) Smith, A. M., Jahn, T. R., Ashcroft, A. E., and Radford, S. E. (2006) Direct Observation of Oligomeric Species formed in the Early Stages of Amyloid Formation using Electrospray Ionization Mass Spectrometry. *J. Mol. Biol. 364*, 9−19.
(38) Smith, D. P., Radford, S. E., and Ashcroft, A. E. (2010) Elongated oligomers in *β*2-microglobulin amyloid assembly revealed by ion mobility spectrometry-mass spectrometry. *Proc. Natl. Acad. Sci. U.S.A. 107*, 6794−6798.
(39) Kloniecki, M., Jablonowska, A., Poznanski, J., Langridge, J., Hughes, C., Campuzano, I., Giles, K., and Dadlez, M. (2011) Ion Mobility Separation Coupled with MS Detects Two Structural States of Alzheimer's Disease Aß1−40 Peptide Oligomers. *J. Mol. Biol. 407*, 110−124.
(40) Englander, S. W. (2006) Hydrogen Exchange and Mass Spectrometry: A Historical Perspective. *J. Am. Soc. Mass Spectrom. 17*, 1481−1489.
(41) Kaltashov, I. A., Engen, J. R., and Gross, M. L. (2006) Hydrogen Exchange and Covalent Modification: Focus on Biomolecular Structure, Dynamics, and Function. 18th Sanibel Conference on Mass Spectrometry. *J. Am. Soc. Mass Spectrom. 17*, i−ii.
(42) Smith, D. L., Deng, Y., and Zhang, Z. (1997) Probing the Noncovalent Structure of Proteins by Amide Hydrogen Exchange Mass Spectrometry. *J. Mass Spectrom. 32*, 135−146.
(43) Busenlehner, L. S., and Armstrong, R. N. (2005) Insights into enzyme structure and dynamics elucidated by amide H/D exchange mass spectrometry. *Arch. Biochem. Biophys. 433*, 34−46.
(44) Lu, X., Wintrode, P. L., and Surewicz, W. K. (2007) *β*-Sheet core of human prion protein amyloid fibrils as determined by hydrogen/deuterium exchange. *Proc. Natl. Acad. Sci. U.S.A. 104*, 1510−1515.
(45) Del Mar, C., Greenbaum, E. A., Mayne, L., Englander, S. W., and Woods, V. L. (2005) Structure and properties of *α*-synuclein and other amyloids determined at the amino acid level. *Proc. Natl. Acad. Sci. U.S.A. 102*, 15477−15482.
(46) Sanchez, L., Madurga, S., Pukala, T., Vilaseca, M., Lopez-Iglesias, C., Robinson, C. V., Giralt, E., and Carulla, N. (2011) A*β*40 and A*β*42 Amyloid Fibrils Exhibit Distinct Molecular Recycling Properties. *J. Am. Chem. Soc. 133*, 6505−6508.
(47) Kheterpal, I., Lashuel, H. A., Hartley, D. M., Walz, T., Lansbury, P. T. J., and Wetzel, R. (2003) A*β* protofibrils possess a stable core structure resistant to hydrogen exchange. *Biochemistry 42*, 14092−14098.
(48) Zhang, A., Qi, W., Good, T. A., and Fernandez, E. J. (2009) Structural Differences between A*β*(1−40) Intermediate Oligomers and Fibrils Elucidated by Proteolytic Fragmentation and Hydrogen/Deuterium Exchange. *Biophys. J. 96*, 1091−1104.
(49) Kheterpal, I., Chen, M., Cook, K. D., and Wetzel, R. (2006) Structural Differences in A*β* Amyloid Protofibrils and Fibrils Mapped by Hydrogen Exchange−Mass Spectrometry with On-line Proteolytic Fragmentation. *J. Mol. Biol. 361*, 785−795.
(50) Rand, K. D., Bache, N., Nedertoft, M. M., and Jørgensen, T. J. D. (2011) Spatially Resolved Protein Hydrogen Exchange Measured by Matrix-Assisted Laser Desorption Ionization In-Source Decay. *Anal. Chem. 83*, 8859−8862.
(51) Zubarev, R. A., Zubarev, A. R., and Savitski, M. M. (2008) Electron Capture/Transfer versus Collisionally Activted/Induced Dissociations: Solo or Duet? *J. Am. Soc. Mass Spectrom. 19*, 753−761.
(52) Coon, J. J. (2009) Collisions or Electrons? Protein Sequence Analysis in the 21st Century. *Anal. Chem. 81*, 3208−3215.
(53) Rand, K. D., Adams, C. M., Zubarev, R. A., and Jørgensen, T. J. D. (2008) Electron Capture Dissociation Proceeds with a Low Degree of Intramolecular Migration of Peptide Amide Hydrogens. *J. Am. Chem. Soc. 130*, 1341−1349.
(54) Zehl, M., Rand, K. D., Jensen, O. N., and Jørgensen, T. J. D. (2008) Electron Transfer Dissociation Facilitates the Measurement of Deuterium Incorporation into Selectively Labeled Peptides with Single Residue Resolution. *J. Am. Chem. Soc. 130*, 17453−17459.
(55) Pan, J., Han, J., Borchers, C. H., and Konermann, L. (2009) Hydrogen/Deuterium Exchange Mass Spectrometry with Top-Down Electron Capture Dissociation for Characterizing Structural Transitions of a 17 kDa Protein. *J. Am. Chem. Soc. 131*, 12801−12808.
(56) Rand, K. D., Zehl, M., Jensen, O. N., and Jørgensen, T. J. D. (2009) Protein Hydrogen Exchange Measured at Single-Residue Resolution by Electron Transfer Dissociation Mass Spectrometry. *Anal. Chem. 81*, 5577−5584.
(57) Landgraf, R. R., Chalmers, M. J., and Griffin, P. R. (2012) Automated Hydrogen/Deuterium Exchange Electron Transfer Dissociation High Resolution Mass Spectrometry Measured at Single-Amide Resolution. *J. Am. Soc. Mass Spectrom. 23*, 301−309.
(58) Huang, R. Y., Garai, K., Frieden, C., and Gross, M. L. (2011) Hydrogen/Deuterium Exchange and Electron-Transfer Dissociation Mass Spectrometry Determine the Interface and Dynamics of Apolipoprotein E Oligomerization. *Biochemistry 50*, 9273−9282.
(59) Konermann, L., Pan, J., and Liu, Y. (2011) Hydrogen Exchange Mass Spectrometry for Studying Protein Structure and Dynamics. *Chem. Soc. Rev. 40*, 1224−1234.
(60) Abzalimov, R. R., Kaplan, D. A., Easterling, M. L., and Kaltashov, I. A. (2009) Protein conformations can be probed in top-down HDX MS experiments utilizing electron transfer dissociation of protein ions without hydrogen scrambling. *J. Am. Soc. Mass Spectrom. 20*, 1514−1517.
(61) Kaltashov, I. A., Bobst, C. E., and Abzalimov, R. R. (2009) H/D Exchange and Mass Spectrometry in the Studies of Protein Conformation and Dynamics: Is There a Need for a Top-Down Approach? *Anal. Chem. 81*, 7892−7899.
(62) Stine, W. B., Jr., Dahlgren, K. N., Krafft, G. A., and LaDu, M. J. (2003) In vitro characterization of conditions for amyloid-*β* peptide oligomerization and fibrillogenesis. *J. Biol. Chem. 278*, 11612−11622.
(63) Xiao, H., Hoerner, J. K., Eyles, S. J., Dobo, A., Voigtman, E., Melcuk, A. I., and Kaltashov, I. A. (2005) Mapping protein energy landscapes with amide hydrogen exchange and mass spectrometry: I. A generalized model for a two-state protein and comparison with experiment. *Protein Sci. 14*, 543−557.
(64) Cech, N. B., and Enke, C. G. (2001) Practical Implication of Some Recent Studies in Electrospray Ionization Fundamentals. *Mass Spectrom. Rev. 20*, 362−387.
(65) Slysz, G. W., Percy, A. J., and Schriemer, D. C. (2008) Restraining Expansion of the Peak Envelope in H/D Exchange-MS and Its Application in Detecting Perturbations of Protein Structure/Dynamics. *Anal. Chem. 80*, 7004−7011.
(66) Kruger, N. A., Zubarev, R. A., Carpenter, B. K., Kelleher, N. L., Horn, D. M., and McLafferty, F. W. (1999) Electron capture versus energetic dissociation of protein ions. *Int. J. Mass Spectrom. 182/183*, 1−5.
(67) Hoerner, J. K., Xiao, H., and Kaltashov, I. A. (2005) Structural and Dynamic Characteristics of a Partially Folded State of Ubiquitin Revealed by Hydrogen Exchange Mass Spectrometry. *Biochemistry 44*, 11286−11294.
(68) Cooper, H. J., Hakansson, K., and Marshall, A. G. (2005) The Role of Electron capture Dissociation in Biomolecular Analysis. *Mass Spectrom. Rev. 24*, 201−222.
(69) Kruger, N. A., Zubarev, R. A., Horn, D. M., and McLafferty, F. W. (1999) Electron capture dissociation of multiply charged peptide cations. *Int. J. Mass Spectrom. 185−187*, 787−793.
(70) Carulla, N., Caddy, G. L., Hall, D. R., Zurdo, J., Gairí, M., Feliz, M., Giralt, E., Robinson, C. V., and Dobson, C. M. (2005) Molecular recycling within amyloid fibrils. *Nature 436*, 554−558.
(71) Baumketner, A., Bernstein, S. L., Wyttenbach, T., Bitan, G., Teplow, D. B., Bowers, M. T., and Shea, J. E. (2006) Amyloid *β*-protein monomer structure: A computational and experimental study. *Protein Sci. 15*, 420−428.
(72) Miranker, A., Robinson, C. V., Radford, S. E., and Dobson, C. M. (1996) Investigation of protein folding by mass spectrometry. *FASEB J. 10*, 93−101.
(73) Kim, M.-Y., Maier, C. S., Reed, D. J., and Deinzer, M. L. (2002) Conformational changes in chemically modified *Escherichia coli* thioredoxin monitored by H/D exchange and electrospray mass spectrometry. *Protein Sci. 11*, 1320−1329.

(74) Krishna, M. M. G., Hoang, L., Lin, Y., and Englander, S. W. (2004) Hydrogen exchange methods to study protein folding. *Methods 34*, 51−64.
(75) Kuprowski, M. C., and Konermann, L. (2007) Signal Response of Co-Existing Protein Conformers in Electrospray Mass Spectrometry. *Anal. Chem. 79*, 2499−2506.
(76) Peschke, M., Verkerk, U. H., and Kebarle, P. (2004) Features of the ESI Mechanism that Affect the Observation of Multiply Charged Noncovalent Protein Complexes and the Determination of the Association Constant by the Titration Method. *J. Am. Soc. Mass Spectrom. 15*, 1424−1434.
(77) Bai, Y., Milne, J. S., Mayne, L., and Englander, S. W. (1993) Primary Structure Effects on Peptide Group Hydrogen Exchange. *Proteins: Struct., Funct., Genet. 17*, 75−86.
(78) Chetty, P. S., Mayne, L., Lund-Katz, S., Stranz, D. D., Englander, S. W., and Phillips, M. C. (2009) Helical structure and stability in human apolipoprotein A-I by hydrogen exchange and mass spectrometry. *Proc. Natl. Acad. Sci. U.S.A. 106*, 19005−19010.
(79) Fersht, A. R. (1999) *Structure and Mechanism in Protein Science*, W. H. Freeman & Co., New York.
(80) Chou, K.-C. (2000) Prediction of Tight Turns and Their Types in Proteins. *Anal. Biochem. 286*, 1−16.
(81) Laganowsky, A., Liu, C., Sawaya, M. R., Whitelegge, J. P., Park, J., Zhao, M., Pensalfini, A., Soriaga, A. B., Landau, M., Teng, P. K., Cascio, D., Glabe, C., and Eisenberg, D. (2012) Atomic view of a toxic amyloid small oligomer. *Science 335*, 1228−1231.
(82) Dupuis, N. F., Wu, C., Shea, J. E., and Bowers, M. T. (2011) The Amyloid Formation Mechanism in Human IAPP: Dimers Have β-Strand Monomer-Monomer Interfaces. *J. Am. Chem. Soc. 133*, 7240−7243.
(83) Liu, T., Pantazatos, D., Li, S., Hamuro, Y., Hilser, V. J., and Woods, V. L. (2012) Quantitative assessment of protein structural models by comparison of H/D exchange MS data with exchange behavior accurately predicted by DXCOREX. *J. Am. Soc. Mass Spectrom. 23*, 43−56.